7-2010

Coherent nonlinear-optical energy transfer and backward-wave optical parametric generation in negative-index metamaterials

Alexander K. Popov
University of Wisconsin - Stevens Point

Sergey A. Myslivets
Siberian Fed Univ

V. M. Shalaev
Birck Nanotechnology Center and School of Electrical and Computer Engineering, Purdue University, shalaev@purdue.edu

Physica B 405 (2010) 2999–3002

Contents lists available at ScienceDirect

Physica B

journal homepage: www.elsevier.com/locate/physb

Coherent nonlinear-optical energy transfer and backward-wave optical parametric generation in negative-index metamaterials

Alexander K. Popov [a,*], Sergey A. Myslivets [b,c], Vladimir M. Shalaev [d]

[a] University of Wisconsin-Stevens Point, 812 Kensington Rd. Neenah, WI 54956, USA
[b] Siberian Federal University, Krasnoyarsk 660041, Russian Federation
[c] Institute of Physics of Russian Academy of Sciences, 660036 Krasnoyarsk, Russian Federation
[d] Birck Nanotechnology Center, Purdue University, West Lafayette, IN 47907, USA

ARTICLE INFO

Keywords:
Negative-index metamaterials
Backward electromagnetic waves
Resonant four-wave mixing and optical parametric amplification
Quantum control

ABSTRACT

The feasibility of all-optically tailored transparency of the negative-index slab, its extraordinary dependence on the intensity of the control field, absorption indices and phase-matching of the parametrically coupled counter-propagating waves is numerically simulated.

1. Introduction

Negative-index (also known as negative phase velocity or left-handed) metamaterials (NIMs) form a novel class of electromagnetic media that promises revolutionary breakthroughs in photonics [1]. Significant progress has been achieved recently in the design of bulk, multilayered, plasmonic structures [2–5]. The majority of NIMs realized to date consist of metal-dielectric nanostructures, meta-atoms, that have highly controllable magnetic and dielectric responses. The challenge, however, is that these structures are strongly lossy. The losses may originate from a number of sources. Irrespective of their origin, losses constitute a major hurdle on the way to practical realization of unique applications of these structures in optics. Therefore, developing efficient loss-compensating techniques is of paramount importance. So far, the most common approaches to compensating losses in NIMs are related with the possibility to embed amplifying centers in the host matrix. The amplification is supposed to be provided through a population inversion between the levels of the embedded centers. Herein, we investigate alternative options based on coherent, nonlinear optical (NLO) energy transfer from the control optical field(s) to the signal through optical parametric amplification (OPA). Nonlinear optics in NIMs remains so far a less-developed branch of optics. On a fundamental level, the NLO response of nanostructured metamaterials is not completely understood or characterized. Nevertheless, it is well established that local-field enhanced nonlinearities can be attributed to plasmonic nanostructures, and some rough estimates of their magnitude can be made. The feasibility of crafting NIMs with strong NLO responses in the optical wavelength range has been experimentally demonstrated in Ref. [6]. Unusual properties of NLO propagation processes in NIMs, such as second-harmonic generation, three-wave mixing (TWM) and four-wave mixing (FWM) OPA, which are in a stark contrast with their counterparts in natural materials, were shown in [7–17]. Striking changes in the properties of nonlinear pulse propagation and temporal solitons [18], spatial solitons in systems with bistability [19–21], gap solitons [22], and optical bistability in layered structures including NIMs [23] were revealed. A review of some of the corresponding theoretical approaches is given in Refs. [24,25]. Herein, we describe basic principles and specific features of the proposed several techniques of compensating losses in NIMs based on nonlinear-optical propagation processes such as coherent three-wave and four-wave mixing in strongly absorbing media. Backwardness of one of the coupled waves (the signal), i.e., opposite direction of its phase velocity and energy flow which is intrinsic to NIMs, is the factor of crucial importance for the proposed techniques.

2. Compensating losses through three-wave-mixing energy-transfer from the control field to the negative-index signal

The basic idea is as follows. Three coupled optical electromagnetic waves with wave vectors $\mathbf{k}_{1,2,3}$ *co-directed* along the z axis propagate through a slab of thickness L with quadratic, TWM, magnetic [8] nonlinearity $\chi^{(2)}$. The outcomes do not change

* Corresponding author.
E-mail addresses: apopov@uwsp.edu (A.K. Popov), sam@iph.krasn.ru (S.A. Myslivets), shalaev@purdue.edu (V.M. Shalaev).

0921-4526/$ - see front matter © 2010 Elsevier B.V. All rights reserved.
doi:10.1016/j.physb.2010.01.022

in the case of electric nonlinearity. Only two waves enter the slab, strong control field at ω_3 and weak signal at ω_1, which then generate a difference-frequency idler at $\omega_2=\omega_3-\omega_1$. The idler contributes back to the signal through the similar TWM process, $\omega_1=\omega_3-\omega_2$, and thus provides OPA of the signal. The signal is assumed negative-index, $n(\omega_1)<0$, and therefore backward wave (BW). This means that the energy flow $\mathbf{S}_1$ is *antiparallel* to $\mathbf{k}_1$ [Fig. 1(a)], which contrasts with the early proposals [26–28] and recent realization [29,30] of BWOPO in PI materials. The idler and the control field are the ordinary waves with parallel $\mathbf{k}_{2,3}$ and $\mathbf{S}_{2,3}$ along the z axis. Consequently, the control beam enters the slab at $z=0$, whereas the signal at $z=L$. Since each point of the medium serves as a source for the generated wave in the backward direction, spatial distribution of the signal and the idler and their output values experience a set of "geometrical" resonances as the functions of gL, which is in stark contrast with those in the ordinary OPA schemes. Then the transmission factor for the backward-wave signal at $z=0$, T_{10} is given by [10,12]

$$T_{10}=\left|\frac{a_1(0)}{a_{1L}}\right|^2=\left|\frac{\exp\{-[(\alpha_1/2)-s]L\}}{\cos RL+(s/R)\sin RL}\right|^2. \quad (1)$$

Here $R=\sqrt{g^2-s^2}$; $s=(\alpha_1+\alpha_2)/4-i\Delta k/2$, $g=(\sqrt{\omega_1\omega_2}/\sqrt[4]{\varepsilon_1\varepsilon_2/\mu_1\mu_2})(8\pi/c)\chi^{(2)}h_3$, h_3 is amplitude of the control field which is assumed homogeneous through the slab, ε_j and μ_j are electric permittivity and magnetic permeability of the slab's material, $\alpha_{1,2}$ are absorption indices at corresponding frequencies. Besides g, a local NLO energy conversion rate for each of the waves is proportional to the amplitude of another coupled wave and depends on the phase mismatch $\Delta k=k_3-k_2-k_1$. Hence, the facts that the waves decay towards opposite directions cause a specific strong dependence of the entire propagation process and, consequently, of the transmission properties of the slab on the ratio of the decay rates. A typical plasmonic NIM slab absorbs about 90% of light at the frequencies which are in the NI frequency-range. Such absorption corresponds to $\alpha_1 L\approx 2.3$. The slab becomes *transparent within the broad range of the slab thickness and the control field intensity* if the transmission in all minimums is about or more than 1. It appeared that such robust transparency can be achieved through the appropriate adjustment of the absorption indices $\alpha_2\geq\alpha_1$ [16]. It is illustrated in Figs. 1(b)–(d). It is seen that the signal grows sharply with the approaching "geometrical" resonances, which indicates *cavityless oscillations*. Fig. 1(f) demonstrates another extraordinary possibility of *eliminating the detrimental effect of the phase-mismatch* by the modest increase of the amplitude of the control field. For $\chi^{(2)}\sim$ 80 pm/V [11] and $P_3\sim$ 15 kW focused to the spot $\emptyset\sim 60\mu$, coupling parameter is estimated as $g\sim 1\mu^{-1}$.

3. Embedded nonlinearity

The above described features allow to propose and to optimize the feasibility of independently engineering the NI and the resonantly enhanced higher-order ($\chi^{(3)}$) NLO response of a composite metamaterial with embedded NLO centers (ions or molecules) [Fig. 2(a) and (b)]. The sample is illuminated by two control fields, E_3 and E_4, so that the amplification of the NI signal, E_1, and the generation of the counter-propagating PI idler, E_2, [Fig. 2(c)] occur due to the FWM process $\omega_1+\omega_2=\omega_3+\omega_4$. The transmission factor for the signal, $T_1(z=0)$ is still described by Eq. (1), where $g^2=g_2^*g_1$, $g_j=\sqrt{|k_1k_2/\varepsilon_1\varepsilon_2|}2\pi\chi_j^{(3)}E_3E_4$, and $\Delta k=k_3+k_4-k_1-k_2$ [13,17]. The schemes in Figs. 2(a) and (b) provide for opposite contributions to the NLO, absorption and refractive indices at ω_1 and ω_2. Hence, according to Figs. 1(b)–(f), the transmission properties for the signal are expected different. All local parameters become strongly dependent on the intensity of the control fields [31] and can be tailored by means of quantum control.

The results of numerical simulations for the example of the scheme in Fig. 2(a) and fully resonant control fields are shown in Fig. 3. Linear and NLO local parameters attributed to the embedded centers are calculated by the density-matrix method

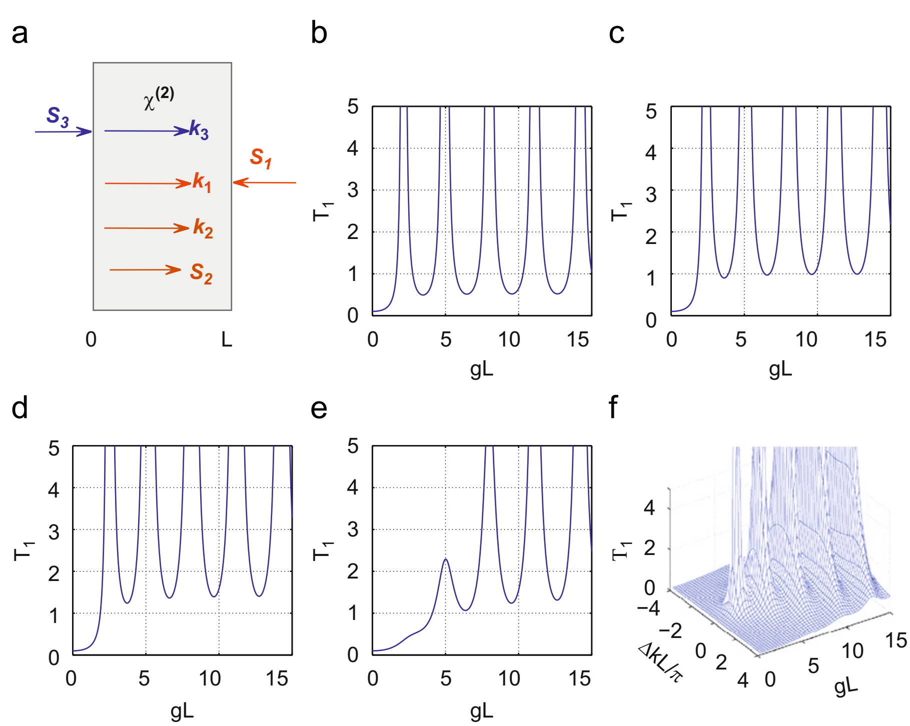

Fig. 1. (a) Coupling geometry. $\mathbf{S}_1$— negative-index signal, $\mathbf{S}_3$— positive-index control field, $\mathbf{S}_2$— positive-index idler. (b)–(f) Transmission $T_1(z=0)$ of the signal at $\alpha_1L=2.3$ and different values of α_2L and ΔkL. (b)–(d) $\Delta k=0$. (b) $\alpha_2L=1$; (c) $\alpha_2L=2.3$; (d)–(f) $\alpha_2L=3$; (e) $\Delta kL=\pi$.

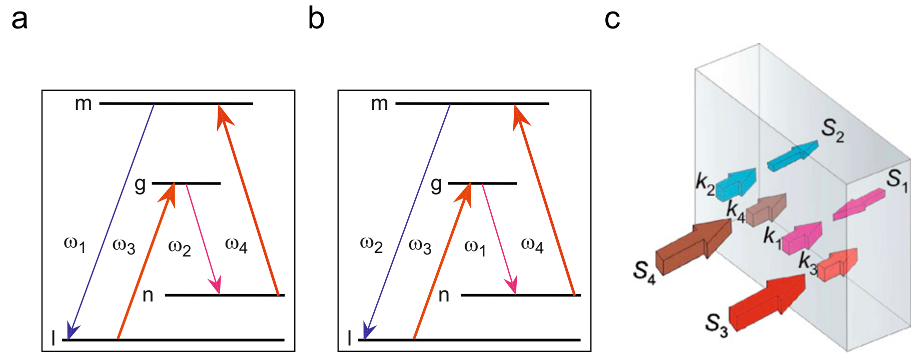

Fig. 2. (a)–(b) Alternative schemes of quantum controlled four-wave mixing in the embedded resonant nonlinear-optical centers with different ratio of the signal and the idler absorption rates and nonlinear susceptibilities. (c) Coupling geometry for four-wave mixing of the backward and ordinary electromagnetic waves. $\mathbf{S}_1$, $\mathbf{k}_1$ and ω_1 are energy flux, wavevector and frequency for the backward-wave signal; $\mathbf{S}_2$, $\mathbf{k}_2$ and ω_2— for the ordinary idler; $\mathbf{S}_{3,4}$, $\mathbf{k}_{3,4}$ and $\omega_{3,4}$— for the ordinary control fields.

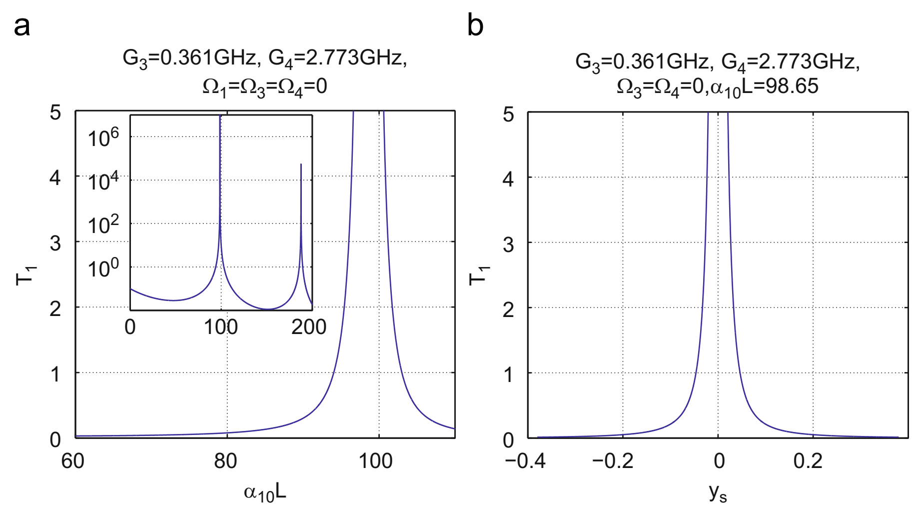

Fig. 3. Transmission of the negative-index signal in the vicinity of the higher frequency transition [Fig. 2(a)], controlled by the fully resonant control fields. $y_s=(\omega_1-\omega_{ml})/\Gamma_{ln}$, $\omega_2=\omega_3+\omega_4-\omega_1$.

as described in Ref. [31]. The strength of the control fields is represented by the coupling Rabi frequencies $G_3=E_3d_{lg}/2\hbar$ and $G_4=E_4d_{nm}/2\hbar$, where d_{ij} are electrodipole transition matrix elements. Resonance offsets for the signal and the idler are denoted as $\Omega_1=\omega_1-\omega_{ml}$, $\Omega_2=\omega_2-\omega_{gn}$. The quantity α_{10} denotes the value of absorption at $\omega_1=\omega_{ml}$ introduced by the embedded centers with all driving fields turned off. The absorption, attributed to the host slab at the frequencies of the signal and the idler, is taken as $\alpha_{h1}L=$ 2.3, and $\alpha_{h2}L=$ 2.1. Relaxation properties of the model are as follows: energy level relaxation rates $\Gamma_n=20$, $\Gamma_g=\Gamma_m=120$; partial transition probabilities $\gamma_{gn}=50$, $\gamma_{mn}=90$ (all in $10^6\,s^{-1}$); homogeneous transition half-widths $\Gamma_{lg}=1$, $\Gamma_{lm}=1.9$, $\Gamma_{ng}=1.5$, $\Gamma_{nm}=1.8$ (all in $10^{11}\,s^{-1}$); $\Gamma_{gm}=5$, $\Gamma_{ln}=0.5$ (all in $10^9\,s^{-1}$); $\lambda_1=756\,nm$ and $\lambda_2=480\,nm$. For the given fields, the ratios of the energy level populations occur $r_l=0.42$, $r_g=0.19$, $r_n=0.2$, $r_m=0.19$ and, hence, no population-inversion or Raman-type gain is involved in the coupling. Fig. 3 proves the feasibility of compensating losses, producing narrow-band transparency, amplification, and mirrorless generation. For the given transitions, the magnitude $G=1\,GHz$ corresponds to the control field intensities of $I\sim 1\,W/(0.1\,mm)^2$. At a resonance absorption cross-section $\sigma_{40}\sim 10^{-16}\,cm^2$, which is typical for transitions with oscillator strength of about one, and a concentration of the embedded centers $N\sim 10^{19}\,cm^{-3}$, one estimates $\alpha_{10}\sim 10^3\,cm^{-1}$ and the required slab thickness in the microscopic range $L\sim(1-100)\,\mu m$. The contribution by the impurities to the refractive index is estimated as $\Delta n<0.5(\lambda/4\pi)\alpha_{40}\sim 10^{-3}$, which essentially does not change the negative refractive index.

4. Conclusion

In conclusion, we have numerically demonstrated the feasibility of the all-optical manipulation of optical properties of NIMs through coherent nonlinear-optical energy transfer from the control to the signal field. The strong nonlinear optical response of the composite can be provided by either the nonlinearity of the building blocks of the negative-index host or by the embedded resonant four-level nonlinear centers. In the latter case, they can be adjusted independently. In addition, we have shown the opportunity for quantum control of the local optical parameters, which employs constructive and destructive quantum interference tailored by two auxiliary driving control fields. Such a possibility is proven with the aid of a realistic numerical model. The investigated features are promising for the compensation of losses in strongly absorbing NIMs, which is the key problem that limits numerous revolutionary applications of this novel class of electromagnetic materials. Among the other possible applications are a novel class of the miniature frequency-tunable narrow-band filters, quantum switchers, amplifiers and cavity-free microscopic optical parametric oscillators that allow the generation of entangled counter-propagating left- and right-handed photons. The unique features of the proposed photonic devices are revealed, such as the strongly resonant behavior with respect to the material thickness, the density of the embedded resonant centers and the intensities of the control fields, the feasibility of negating the linear phase-mismatch introduced by the host material, and the role of absorption or, conversely, the supplementary nonparametric amplification of the idler.

Acknowledgments

This work was supported by the U.S. Army Research Laboratory and by the U.S. Army Research Office under Grants number W911NF-0710261 and 50342-PH-MUR and by the Siberian Division of the Russian Academy of Sciences under Integration Project no. 5 and by the Presidium of the Russian Academy of Sciences under Grant No 27.1.

References

[1] V.M. Shalaev, Nat. Photonics 1 (2007) 41.
[2] C.M. Soukoulis, M. Kafesaki, Weakly and strongly coupled optical metamaterials, Invited talk at the Nanometa 2009, The 2nd European Topical Meeting on Nanophotonics and Metamaterials, 5–8 January, Seefeld, Tirol, Austria, 2009.
[3] N. Katsarakis, G. Konstantinidis, A. Kostopoulos, R.S. Penciu, T.F. Gundogdu, M. Kafesaki, E.N. Economou, T. Koschny, C.M. Soukoulis, Opt. Lett. 30 (2005) 1348.
[4] X. Zhang, Optical bulk metamaterials, Plenary talk at the Nanometa 2009, The 2nd European Topical Meeting on Nanophotonics and Metamaterials, 5–8 January, Seefeld, Tirol, Austria, 2009.
[5] J. Valentine, S. Zhang, T. Zentgraf, E. Ulin-Avila, D.A. Genov, G. Bartal, X. Zhang, Nature 455 (2008) 376.
[6] M.W. Klein, M. Wegener, N. Feth, S. Linden, Experiments on second- and third-harmonic generation from magnetic metamaterials, Opt. Exp. 15 (2007) 5238; Erratum 16 (2008) 8055.
[7] V.M. Agranovich, Y.R. Shen, R.H. Baughman, A.A. Zakhidov, Phys. Rev. B 69 (2004) 165112(7).
[8] I.V. Shadrivov, A.A. Zharov, Y.S. Kivshar, J. Opt. Soc. Am. B 23 (2006) 529.
[9] A.K. Popov, V.V. Slabko, V.M. Shalaev, Laser Phys. Lett. 3 (2006) 293.
[10] A.K. Popov, V.M. Shalaev, Appl. Phys. B 84 (2006) 131.
[11] M. Scalora, G. D'Aguanno, M. Bloemer, M. Centini, D. de Ceglia, N. Mattiucci, Y.S. Kivshar, Opt. Exp. 14 (2006) 4746.
[12] A.K. Popov, V.M. Shalaev, Opt. Lett. 31 (2006) 2169.
[13] A.K. Popov, S.A. Myslivets, T.F. George, V.M. Shalaev, Opt. Lett. 32 (2007) 3044.
[14] A.K. Popov, S.A. Myslivets, V.M. Shalaev, Appl. Phys. B Lasers Opt. 96 (2009) 315.
[15] A.K. Popov, S.A. Myslivets, V.M. Shalaev, Opt. Lett. 34 (2009) 1165.
[16] A.K. Popov, S.A. Myslivets, Appl. Phys. Lett. 93 (2008) 191117(3).
[17] A.K. Popov, S.A. Myslivets, V.M. Shalaev, J. Opt. A Pure Appl. Opt. 11 (2009) 114028(13).
[18] N. Lazarides, G.P. Tsironis, Phys. Rev. E 71 (2005) 036614(4).
[19] P. Tassin, L. Gelens, J. Danckaert, I. Veretennicoff, G.V. der Sande, P. Kockaert, M. Tlidi, Chaos Interdisciplinary J. Nonlinear Sci. 17 (2007) 037116(11).
[20] P. Kockaert, P. Tassin, G.V. der Sande, I. Veretennicoff, M. Tlidi, Phys. Rev. A 74 (2006) 033822(8).
[21] A. Boardman, N. King, R. Mitchell-Thomas, V. Malnev, Y. Rapoport, Metamaterials 2 (2008) 145–154 metamaterials'2007 Congress.
[22] G. D'Aguanno, N. Mattiucci, M. Scalora, M.J. Bloemer, Phys. Rev. Lett. 93 (2004) 213902(4).
[23] N.M. Litchinitser, I.R. Gabitov, A.I. Maimistov, V.M. Shalaev, Opt. Lett. 32 (2007) 151.
[24] A. Maimistov, I. Gabitov, Nonlinear optical effects in artificial materials, in: J.-G. Caputo, M.P. Soerensen (Eds.), European Physics Journal Special Topics: Nonlinear Waves in Complex Systems: Energy Flow and Geometry, vol. 147, Springer, Berlin, 2007, pp. 265–286.
[25] N.M. Litchinitser, I.R. Gabitov, A.I. Maimistov, V.M. Shalaev, Negative refractive index metamaterials in optics, in: E. Wolf (Ed.), Progress in Optics, vol. 51, Elsevier, Amsterdam, 2007, pp. 1–68.
[26] S.E. Harris, Appl. Phys. Lett. 9 (1966) 114.
[27] K.I. Volyak, A.S. Gorshkov, Radiotekhnika i Elektronika (Radiotechnics and Electronics) 18 (1973) 2075 (in Russian).
[28] A. Yariv, Quantum Electronics, second ed., Wiley, New York, 1975 (Chapter 18).
[29] C. Canalias, V. Pasiskevicius, Nat. Photonics 1 (2007) 459.
[30] J.B. Khurgin, Nat. Photonics 1 (2007) 446.
[31] A.K. Popov, S.A. Myslivets, T.F. George, Phys. Rev. A 71 (2005) 043811(13).